

1 **Improving growth estimates for western Atlantic Bluefin tuna using an integrated modeling**
2 **approach.**

3
4 Lisa E. Ailloud^{a,*}, Matthew V. Lauretta^b, Alex R. Hanke^c, Walter J. Golet^d, Robert J. Allman^e, Matthew
5 R. Siskey^f, David H. Secor^g, John M. Hoenig^h

6
7 ^a Virginia Institute of Marine Science, College of William & Mary, P.O. Box 1346, Gloucester Point, VA 23062, U.S.A.,
8 lailloud@vims.edu, *Corresponding author

9 ^b National Marine Fisheries Service, Southeast Fisheries Science Center, 75 Virginia Beach Drive, Miami, FL 33149, U.S.A.,
10 matthew.lauretta@noaa.gov

11 ^c Department of Fisheries and Oceans Canada, 531 Brandy Cove Rd, St. Andrews, New Brunswick, Canada,
12 alex.hanke@dfo-mpo.gc.ca

13 ^d School of Marine Sciences at the University of Maine & Gulf of Maine Research Institute, 350 Commercial Street,
14 Portland, ME 04101, U.S.A., walter.golet@maine.edu

15 ^e National Marine Fisheries Service, Southeast Fisheries Science Center, 3500 Delwood Beach Rd, Panama City, FL 32408,
16 U.S.A., robert.allman@noaa.gov

17 ^f Stony Brook University, School of Marine and Atmospheric Sciences, Stony Brook, NY 11794, U.S.A.,
18 matthew.siskey@stonybrook.edu

19 ^g Chesapeake Biological Laboratory, University of Maryland Center for Environmental Science, Solomons, MD 20688,
20 U.S.A., secor@umces.edu

21 ^h Virginia Institute of Marine Science, College of William & Mary, P.O. Box 1346, Gloucester Point, VA 23062, U.S.A.,
22 hoenig@vims.edu

23
24
25 **Abstract**

26 Advances in modeling growth using tag-recapture data and progress in otolith ageing procedures
27 allowed improved fitting of the western Atlantic bluefin tuna growth curve. Growth parameters were
28 derived from an integrated analysis of tag-recapture data and otolith age-length data using the “Aires-da-
29 Silva-Maunders-Schaefer-Fuller with correlation” (AMSFc) framework, which models growth such that
30 parameter estimates from each data source are directly comparable. The otolith data consisted of a
31 sample of 4,045 otoliths for which ages were estimated using tested and consistent protocols and
32 conventions designed to avoid bias. Strict data quality control measures were applied to the tagging data
33 for quality assurance and a subsample of 1,118 records were retained for use in the analysis. Two forms
34 of the Schnute (1981) growth model were considered: the Richards model and the von Bertalanffy
35 model. The Richards curve appears to provide a better fit. Both curves follow a similar trajectory until
36 age 16, after which they diverge considerably. The Richards model supports a lower mean asymptotic
37 length (L_{∞} = 271.0 cm FL) than the model currently used in the stock assessment (L_{∞} = 314.9 cm FL).

38 **Keywords:** Growth, *Thunnus thynnus*, fisheries stock assessment, otolith, tagging.

39

1. Introduction

Migratory pelagic fish present both opportunities and challenges in developing predictive growth models. Species such as Atlantic bluefin tuna *Thunnus thynnus* (ABT) attract substantial fishing effort, affording opportunities to access fish for tagging and collection of otoliths, which support parameterization of growth. Principal challenges include sufficient sampling, implementing quality control procedures to curtail biased observations throughout the stock's range, and making best use of combined age-length and tag-recapture data. Otolith data are used to estimate absolute ages and allow size-at-age functions to be modeled. For western ABT, these data are largely centered on the larger/older fish targeted by the recreational and commercial fisheries. Tagging data often have the opposite problem of lacking large fish and fish with long times at liberty. Each data source is also prone to various sources of observation error – mainly variability in age assignment across readers and measurement error in recorded fish lengths. It is therefore advantageous to estimate growth from both sources of data simultaneously to increase the size and representativeness of the sample and test the influence of each dataset on resulting parameter estimates (Maunder and Punt, 2013). We apply a new maximum likelihood approach to fit jointly direct age estimates, for a large sample of otoliths, with release and recapture lengths of conventionally-marked fish.

ABT is the largest member of the Scombridae family. It can reach weights exceeding 600 kg (Collette and Nauen, 1983) and live over 34 years (present study). The species is assessed and managed as two distinct stocks by the International Commission for the Conservation of Atlantic Tunas (ICCAT) under the assumption of no net mixing (ICCAT, 2014): the eastern stock (eastern Atlantic/Mediterranean) and the western stock (western Atlantic/Gulf of Mexico), with spawning grounds on opposite sides of the North Atlantic Ocean basin (Boustany et al., 2008; Carlsson et al., 2007; Riccioni et al., 2010; Richardson et al., 2016). Although these two stocks are conventionally separated by the 45°W meridian, tagging data indicate a high degree of transoceanic migration for animals of all ages, with significant mixing occurring on foraging grounds (Block et al., 2001, 2005; Sibert et al., 2006).

Following years of overfishing, ICCAT adopted rebuilding plans for the western and eastern stocks in 1998 and 2006, respectively, gradually tightening control measures over time, as the Commission strived to meet its objectives. According to the latest stock assessment, both stocks are showing signs of recovery. Still, considerable uncertainties remain in the assessment, particularly regarding maturity, growth dynamics and the level of mixing between the two stocks, making it difficult to draw definite conclusions about the current and future status of the stock (ICCAT, 2014).

Information on age and growth is needed to assess properly a depleted stock and define its rebuilding target. This holds especially true for bluefin tuna for which a growth curve is used to translate catch-at-size to catch-at-age through cohort slicing in the stock assessment process. Being a moderately long-lived, iteroparous species, bluefin tuna relies on the periodic production of strong year classes to persist through time (Secor, 2007). In this case, it becomes particularly important to characterize precisely the age structure of the stock, since having a truncated age structure (Siskey et al., 2016) and being the target of a highly age/size selective fishery (ICCAT, 2014) can severely compromise the sustainability of the fishery.

The growth parameters currently used in the assessment of western ABT (Restrepo et al., 2010) were derived from a combination of otolith-based age readings for large fish (n=146; Neilson and Campana, 2008; Secor et al., 2009) and modal analysis of length frequency data for small fish (1-3 years of age, 1970's US purse seine data). In their analysis, Restrepo et al. (2010) did not include information available in the ICCAT tagging database used to construct the former growth curve (Turner and Restrepo, 1994) due to data quality concerns and biases in the estimation process. Although the Restrepo

86 et al. (2010) analysis was a significant improvement over the former growth curve, recent advances in
87 integrative modeling and otolith age reading techniques highlights the need for an updated assessment of
88 the current growth curve.

89 During a workshop aimed at standardizing otolith-based ageing protocols for ABT, Busawon et al.
90 (2015) determined that the otoliths used by Restrepo et al. (2010) were significantly over-aged (average
91 3 years) due to errors in assignment of the first annulus. The problem was resolved using a standardized
92 reference scale for the first annulus adopted by the laboratories involved in ageing studies (Secor et al.,
93 2014a).

94 Improvements in both data quality control (Ailloud et al., 2014) and modeling techniques (Aires-da-
95 Silva et al., 2015; Francis et al., 2016) now allow for the ICCAT tagging data to be incorporated in the
96 growth analysis. Francis (1988) showed that growth parameters estimated from age-length data and
97 tagging data have different interpretations when tagging data are analyzed by modeling growth
98 increments through time (e.g., as done by Fabens, 1965). Comparing these estimates assumes that the
99 expected annual growth of fish of age A (estimated from age-length data) is equivalent to the expected
100 annual growth of fish whose length is equal to the mean length of fish of age A (estimated from tagging
101 data), which is seldom the case (Francis, 1988). In recent years, maximum likelihood approaches have
102 been developed that model the joint density of the release and recapture lengths as a function of age,
103 making growth estimates age-based and thus avoiding the comparability problem (Laslett et al., 2002;
104 Palmer et al., 1991; Wang et al., 1995). At the forefront of integrated methods is the so-called “Laslett-
105 Eveson-Polacheck” (LEP) approach (Eveson et al., 2004), which models the release and recapture
106 lengths as functions of age by treating age at tagging and asymptotic length, L_{∞} , as random variables.
107 Though statistically attractive, this method can be difficult to implement due to its high computational
108 demands and complicated error structures. A simpler alternative was developed by Aires-da-Silva et al.
109 (2015) and later improved upon by Francis et al. (2016) by allowing correlation among deviates in
110 tagging length: the AMSFc approach (Francis et al., 2016), named after Aires-da-Silva, Maunder,
111 Schaefer and Fuller, where ‘c’ stands for correlation. Like the LEP approach, this method also treats
112 pairs of observed lengths as a function of age, but treats L_{∞} as a fixed parameter, greatly reducing the
113 computational demands of the model (Aires-da-Silva et al., 2015). The AMSFc approach is applied here
114 to fit and compare alternative growth models for the western stock of ABT.

115 2. Materials and Methods

116 2.1 Tagging data

117 The ICCAT conventional tagging database combines tag release and return information from several
118 tagging studies conducted in various regions of the North Atlantic Ocean over the past 75 years. Of
119 more than 85,000 releases, ICCAT recovered information for nearly 6,000 recaptures, of which 2,434
120 had complete and plausible data (e.g., non-negative times at liberty) on the date and length at release and
121 recapture. Ailloud et al. (2014) demonstrated that the database contains valuable information for
122 estimating growth of bluefin tuna (such as records of fish that were at liberty for many years and of old
123 fish which appear to have reached their maximum sizes), but that extraction of the data must be done
124 with care. Quality control measures employed in our analysis are detailed below (applied to data from
125 the 06/30/2016 database update).

- 126 1) Animals at liberty for less than 105 days (~3.5 months) were excluded from the analysis
127 (1,068 records) since, a) for fish with short times at liberty, the observed growth increments
128 largely represent measurement error rather than somatic growth (Ailloud et al., 2014), and b)
129 stress related to the tagging event could potentially have an adverse effect on growth in the
130 short run.

- 131 2) Records showing the fastest and slowest 2% absolute growth per day were removed in an
132 attempt to eliminate outliers (i.e., data entry misrecordings and large measurement errors) and
133 improve growth parameter estimates (116 records dropped). To test the sensitivity of the
134 results to these outliers, a separate run that included the outliers was performed.
- 135 3) Fish both captured and recaptured in the eastern Atlantic, as well as fish either captured or
136 recaptured in the Mediterranean, were excluded from the analysis (132 records). This rule
137 does not guarantee that fish of eastern origin are removed from the sample since considerable
138 mixing is known to occur (Siskey et al., 2016), but it instead attempts to keep the tagging data
139 sample focused on fish present in the western Atlantic, since growth is presumably linked to
140 local conditions (e.g., prey abundance, water temperature and fish density).

141
142 The resulting dataset consisted of 1,118 records with lengths at tagging ranging from 36 cm FL to
143 259 cm FL, lengths at recapture ranging from 53 cm FL to 292 cm FL (Supplementary Fig. A1) and
144 times at liberty ranging from 4.5 months to 16 years (median= 1 year). 53% of the records corresponded
145 to fish tagged in the 1960's, another 43% corresponded to fish tagged in the 1970's and the remaining
146 4% were released between 1980 and 2011.

147 2.2 Otolith data

148 The otolith data consisted of samples collected from the Gulf of Mexico (n=305), the southeastern
149 USA (n=55), the USA Mid-Atlantic Bight (n=1,141) and the Northeastern USA/Canada (n=2,512)
150 (Supplementary Fig. A2). The large majority of otoliths (85%) was collected between 2009 and 2015.
151 Snout lengths and curved fork lengths (CFL) were converted to straight fork lengths (FL) using
152 conversion factors from Secor et al. (2014b) and Rodriguez-Marin et al. (2015), respectively. In the few
153 cases where no length measurements were taken (3.5% of records), round weights were converted to FL
154 using monthly conversion factors from Rodriguez-Marin et al. (2015). Sizes ranged from 48 cm FL to
155 300 cm FL (Supplementary Fig. A1) and age estimates from 1 to 34 years.

156 Neilson and Campana (2008) validated absolute age in large/old bluefin tuna using bomb
157 radiocarbon dating and Siskey et al. (2016) confirmed the annual periodicity of growth increments,
158 validating otolith ageing for the species. Otolith samples were prepared and read by experts following
159 the standardized protocol outlined in Secor et al. (2014a) and Busawon et al. (2015) which, among other
160 things, prescribes using a reference scale to identify the first annulus and performing multiple reads per
161 otolith to detect any inconsistencies and reduce ageing error. Using a reference set of otoliths (n=100),
162 Busawon et al. (2015) estimated that ageing error was low among readers and detected no systematic
163 bias. Each sample was assigned an integer age based on annuli counts of either opaque or translucent
164 bands, which was then adjusted (a_{adj}) to account for the timing of band formation (i.e. when counting
165 opaque bands, one year was added to the age if the fish was caught between January and June; when
166 counting translucent bands, one year was deducted from the age if the fish was caught between July and
167 December. The estimated age was then assigned a decimal age (a_{final}) that accounted for the time
168 elapsed between birth month (b) and month of capture (c) using the following equation:

169

$$a_{final} = a_{adj} + (c - b)/12 \quad (1)$$

170

171 To test the influence of outliers on the resulting parameter estimates, a sensitivity run analysis was
172 performed by excluding otolith records whose length observations fell beyond 3 standard deviations
173 from the mean for each age (33 records). Additionally, because of the possibility that the size
174 composition of the first few age groups was positively biased by a combination of size selectivity of the

175 fishery (only the largest individuals at age 1 and 2 are caught owing to a minimum size limit of 6.4 kg
 176 established in 1975) and timing of capture (all fish ages 1 and 2 were captured in the summer months
 177 when growth is thought to be fastest; Supplementary Fig. A2) the growth models were refitted without
 178 age groups 1 and 2.

179 2.3 The AMSFc approach

180 We used the AMSFc approach of Francis et al. (2016) to analyze the otolith and tagging data
 181 simultaneously. This maximum likelihood method has two likelihood components, one for each data
 182 source, both of which model length as a function of age. For the tagging data, this entails modeling the
 183 joint distribution of the lengths-at-release and –at-recapture (with correlation ρ) as a function of age at
 184 tagging (A_{tag}) and time at liberty (Δt). Since A_{tag} is unknown, it is treated as a random effect with an
 185 assumed probability distribution whose parameters are estimated in the maximum likelihood framework.
 186 For each component, a common growth function is specified to describe the relationship between mean
 187 length and age, and variability in length-at-age is defined.

188 2.4 The growth function

189 Two growth models were considered to describe the functional relationship between fish length (L)
 190 and age (a): the Richards (1959) model and the von Bertalanffy (1938) model. The von Bertalanffy
 191 model was chosen to allow for a direct comparison of the results to the growth curve currently used in
 192 the stock assessment (i.e., Restrepo et al., 2010) and the Richards model was chosen for its increased
 193 flexibility in fitting data. The Richards function has an additional shape parameter (p) that allows it to
 194 take on a sigmoidal form. Let A_1 and A_2 be two reference ages (pre-specified by the modeler) with
 195 corresponding mean lengths L_1 and L_2 , respectively, and p be a shape parameter ($p \leq 1$). Then, both
 196 models can be expressed as special cases of the Schnute (1981) model, as follows:
 197

$$L_a = f(a; \theta = \{p, K, A_1, A_2, L_1, L_2\}) \quad (2)$$

198 where,

$$f(a; \theta) = [L_1^p + (L_2^p - L_1^p) \frac{1 - e^{-K(a-A_1)}}{1 - e^{-K(A_2-A_1)}}]^{1/p} \quad (3)$$

199 While growth models are typically parameterized in terms of L_∞ and t_0 (the theoretical age at size 0),
 200 the Schnute model is parameterized in terms of two reference ages, A_1 and A_2 , representing the youngest
 201 and oldest fish in the sample, respectively. This parameterization reduces the correlation between the
 202 estimates of parameters, unlike models parameterized in terms of L_∞ and K , which are otherwise highly
 203 correlated. The shape parameter, p , is related to the ratio of the length at the inflection point to the mean
 204 asymptotic length (L_∞). When $p = 1$, there is no inflection point and the model reverts to a von
 205 Bertalanffy curve. When $p < 1$ it takes on the shape of a Richards curve, with the inflection point
 206 moving up along the age-length curve as p decreases. K has units time^{-1} , when an inflection point exists,
 207 its inverse, $1/K$, is related to the age associated with the inflection point on the curve. For the von
 208 Bertalanffy model, K relates to the rate of approach to the asymptote. Schnute (1981) provides the
 209 following equations to obtain L_∞ and t_0 from the parameters of the Schnute model:
 210

$$L_\infty = \left[\frac{e^{KA_2} L_2^p - e^{KA_1} L_1^p}{e^{KA_2} - e^{KA_1}} \right]^{1/p} \quad (4)$$

$$t_0 = A_1 + A_2 - \frac{1}{K} \ln \left[\frac{e^{KA_2} L_2^p - e^{KA_1} L_1^p}{L_2^p - L_1^p} \right] \quad (5)$$

211

212 Variability about the mean length-at-age was modelled as the sum of process error (i.e. true
 213 variability around the mean curve resulting from individual variability in growth) and observation error
 214 (i.e. resulting from estimated or converted length measurements). As in Aires-da-Silva et al. (2015), true
 215 variability around the mean curve (hereafter referred to as “variability in length at age”) was defined as a
 216 linear function of length with intercept a^* and slope b ,

$$\sigma_{L_a} = a^* + bL_a \quad (6)$$

217 while observation error, σ_{obs} , was defined as,
 218

$$\sigma_{obs} = \sigma_{obs} I_i \quad (7)$$

219 where I_i is an indicator variable that takes on the value 1 if a length record was either estimated or
 220 converted from another length/weight measurement and 0 if it was directly measured as straight FL.

221 2.5 Otolith likelihood

222 The log-likelihood for the otolith data, $\ln(\lambda_{oto})$, was expressed as the sum of the log-likelihood
 223 contributions from each fish. Length-at-age was assumed to be normally distributed with expected
 224 length given by (1). To avoid computational problems, the linear relationship of the variability in length-
 225 at-age with length (eq. 7) was parameterized in terms of the reference lengths L_1 and L_2 (estimated by the
 226 model), as follows (Schnute and Fournier, 1980):

$$\sigma_{L_a} = \sigma_{L_1} + (\sigma_{L_2} - \sigma_{L_1}) \frac{E[L_a] - L_1}{L_2 - L_1} + \sigma_{obs} I_i \quad (8)$$

227 2.6 Tag-recapture likelihood

228 Lengths-at-tagging and –at-recapture were modeled following a bivariate normal distribution with
 229 correlation, ρ . The expected length at age of individual fish was defined by the expected lengths at
 230 tagging (L_{tag}) and recapture (L_{rec}), given the unknown age at tagging (A_{tag}) and time spent at liberty
 231 between each capture event (Δt) (i.e., $f()$ given in eq.2):
 232

$$E[L_{tag}|A_{tag} = a] = f(A_{tag} = a; \theta) \quad (9.1)$$

$$E[L_{rec}|a + \Delta t] = f(a + \Delta t; \theta) \quad (9.2)$$

233 The random effects for the age-at-tagging (A_{tag}) were assumed to follow a lognormal distribution
 234 with mean ($\mu_{\log A_{tag}}$) and standard deviation ($\sigma_{\log A_{tag}}$) of A_{tag} estimated on the log scale. The
 235 lognormal distribution was chosen because it seemed to provide a reasonable approximation to the
 236 distribution of lengths-at-release. Given the small sizes and narrow size range observed in the length-at-
 237 release, we expected a relatively linear relationship between length-at-age and length-at-release. As with
 238 the otolith data, the standard deviations associated with each length were defined as:
 239
 240

$$\sigma_{L_{tag}} = \sigma_{L_1} + (\sigma_{L_2} - \sigma_{L_1}) \frac{E[L_{tag}|a] - L_1}{L_2 - L_1} + \sigma_{obs} I_i \quad (10.1)$$

$$\sigma_{L_{rec}} = \sigma_{L_1} + (\sigma_{L_2} - \sigma_{L_1}) \frac{E[L_{rec}|a + \Delta t] - L_1}{L_2 - L_1} + \sigma_{obs} I_i \quad (10.2)$$

241 As Francis et al. (2016) demonstrated, lengths-at-tagging and –at-recapture are likely to be more
 242 highly correlated when time-at-liberty is short ($\text{cor}(L_{tag}, L_{rec})$ close to 1), with correlation decreasing
 243

244 with increasing time at liberty. Thus, the correlation coefficient, ρ , was modeled as a simple decreasing
 245 function of Δt (Francis et al., 2016):
 246

$$\rho = 1 - \frac{1 - \rho_0}{1 - \rho_0 + \rho_0 e^{(-k_\rho \Delta t)}} \quad (11)$$

247 where ρ_0 ($0 < \rho_0 < 1$) is the correlation between L_{tag} and L_{rec} when $\Delta t = 0$, and k_ρ ($k_\rho > 0$) is related
 248 to the steepness of the slope defining the relationship between ρ and Δt (the higher the value of k_ρ , the
 249 faster the correlation coefficient will decline to zero).
 250

251 The overall tagging log-likelihood, $\ln(\lambda_{tag})$, was the sum of the bivariate normal log-likelihood of
 252 L_{tag} and L_{rec} and the lognormal log-likelihood of the random effects.

253 2.7 Objective function

254 The log-likelihoods of the tagging data and otolith data were added together into one objective
 255 function to be optimized:
 256

$$\Lambda = \ln(\lambda_{oto}) + \ln(\lambda_{tag}) \quad (12)$$

257 The optimization was carried out in ADMB-RE (Fournier et al., 2012) using the separable functions
 258 feature to reduce memory requirements and computational demand of the random effects (Skaug and
 259 Fournier, 2015). The program's default convergence criterion (maximum gradient component $< 10^{-4}$)
 260 was used to evaluate convergence at the optimal solution. Due to differences in sample sizes between
 261 the two datasets, the otolith data carried more weight than the tagging data on the overall analysis. A
 262 sensitivity run was therefore conducted to test whether down-weighting the influence of the otolith data
 263 caused any noticeable changes to the results. The otolith log-likelihood was multiplied by a factor of
 264 0.27, the inverse of the 3.7 times as many otolith records as tagging records.
 265

266 2.8 Model diagnostics

267 Goodness of fit was first determined by visual inspection of the data plotted against the fitted curve.
 268 For the otolith data, a scatterplot of the standardized residuals was produced to look for any indication of
 269 poor model fit. Interpreting the residuals of the tagging component was complicated by the correlation
 270 between the lengths-at-tagging and -at-recapture. Instead a comparison was made between the observed
 271 lengths-at-recapture and their expected distributions given the parameters estimated in the model. This
 272 was done by calculating the conditional cumulative distribution function (c.d.f.) of L_{rec} given L_{tag} and
 273 Δt using the following approximation (see Appendix in Francis et al. (2016) for a detailed derivation):

$$F_{L_{rec},i}(L_{rec} | L_{tag} = L_{tag,i}, \Delta t = \Delta t_i) \approx \frac{\sum_j [F_{L_{rec},i}(L_{rec} | L_{tag} = L_{tag,i}, \Delta t = \Delta t_i, A_{tag} = A_j) f_{L_{tag},i}(L_{tag} | A_{tag} = A_j) f_{A_{tag}}(A_j)]}{\sum_j [f_{L_{tag}}(L_{tag} | A_{tag} = A_j) f_{A_{tag},i}(A_j)]} \quad (1)$$

274 where F_X denotes the c.d.f. of X , f_X denotes the probability density function (p.d.f.) of X , i refers to
 275 individual fish in the dataset, and $\{A_j\}$ is a large set of equally spaced numbers covering the expected
 276 range of ages at tagging. If the model fits the tagging data, we would expect the quantiles of the
 277 conditional distribution to be evenly distributed over the interval (0,1). A Kolmogorov-Smirnov test was
 278 also carried out to formally compare the quantiles with that of a uniform distribution.

279 Finally, a log likelihood ratio test (with 1 degree of freedom and a significance level of $\alpha=0.05$) was
280 used to determine whether the addition of the shape parameter in the Richards model provided a
281 significant improvement in fit over the simpler von Bertalanffy model.

282 3. Results

283 The two models generally follow similar growth trajectories until age 16 (~250cm FL), with the
284 Richards model predicting slightly larger lengths for fish of ages 7 to 16 compared to the von
285 Bertalanffy model (Table 1; Supplementary Fig. A3). Beyond age 16, the two curves begin to diverge
286 considerably, with the von Bertalanffy model predicting a higher mean asymptotic length ($L_{\infty} = 318.9$
287 cm FL) than the Richards model ($L_{\infty} = 271.0$ cm FL) (Supplementary Fig. A3). There were also notable
288 differences in the estimates of variability in length-at-age between the two models: the von Bertalanffy
289 model predicted smaller variability in length-at-age for younger fish ($\sigma_{L_1} = 5.0 < 7.7$ cm FL) and higher
290 variability in length-at-age for older fish ($\sigma_{L_2} = 29.1 > 21.0$ cm FL), compared with the Richards model.
291 The von Bertalanffy growth curve currently used in the western ABT stock assessment (Restrepo et al.,
292 2010) was very similar to that estimated here (Supplementary Fig. A3).

293 Visual inspection of the fitted curve against the otolith data (Fig. 1) indicated that the Richards
294 model was a better fit than the von Bertalanffy model. Although the data show evidence of an
295 asymptote, the von Bertalanffy model is not able to adequately capture the bend in the curve (Fig. 1).
296 The scatterplot of residuals (Fig. 2) confirms this. The von Bertalanffy model displays a strong negative
297 pattern in the residuals beyond age 18 (Fig. 2) that is only weakly apparent in the residual plot of the
298 Richards model (beyond age 22; Fig. 2). There is a noticeable lack of very young fish in the otolith data
299 (Fig. 1), and both model fits show a positive trend in the residuals of fish aged 1-3, that is slightly more
300 pronounced in the Richards model (Fig. 2). In the von Bertalanffy fit, there is a negative pattern to the
301 residuals for fish of ages 4-6 followed by a positive pattern in the residuals of fish ages 7-16.

302 The fit to the tagging data seemed adequate and similar between the two models (Fig. 3).
303 Trajectories of fish with long times at liberty were in agreement with the general trajectory of the growth
304 curve (Fig. 3) and both models estimated similar values for the parameters of the lognormal distribution
305 of the unknown ages at tagging (Table 1, Fig. 4). The few records of fish that were relatively large at the
306 time of release may have been under-aged (Fig. 3) but their influence on the results was negligible since
307 they represented just 1% of the total tagging data sample. The histograms of quantiles of the conditional
308 distribution of $(L_{rec}|L_{tag}, \Delta t)$ (Fig. 5) indicated that the von Bertalanffy model provided a slightly better
309 fit to the tagging data than the Richards model. The differences in fit were a result of fish being assigned
310 slightly younger ages at tagging under the von Bertalanffy model compared to the Richards model.
311 Nonetheless, results from the Kolmogorov-Smirnov tests indicated that both models had some level of
312 misfit since the quantile distributions associated with each model were both significantly different from
313 a uniform distribution (p-value<0.01). These differences in fit between the two models are relatively
314 unimportant when compared to the differences in fits observed in the otolith data. Trends in the otolith
315 residuals resulting from the von Bertalanffy model were indicative of a much greater problem. Results
316 from the likelihood ratio test likewise indicated that the Richards parameterization was a better fit to the
317 data than the simpler von Bertalanffy parameterization (p-value<0.001). Therefore, the Richards curve
318 appears to be superior to the von Bertalanffy curve for modelling the growth of western ABT.

319 Down-weighting the otolith component of the likelihood did not make an appreciable difference in
320 the resulting curve for either model (Supplementary Fig. A4, Table A1). This indicates that the otolith
321 and tagging data are complementary and in agreement with one another. What did change as a result of
322 shifting the weight away from the otolith data were changes in the estimates of variability in length-at-
323 age estimates. The Richards model with down-weighted otolith component estimated smaller variability

324 in length at young ages ($\sigma_{L_1} = 2.03 \pm 0.5 < 7.7 \pm 0.6$) and larger variability at older ages ($\sigma_{L_2} = 27.9 \pm 1.2$
325 $> \sigma_{L_2} = 21.0 \pm 0.7$) compared to the Richards model without weights (Supplementary Table A1).

326 The decision to exclude tagging records of fish showing the slowest and fastest 2% growth did not
327 make any appreciable difference to the results (Supplementary Table A1). For the otolith data, the
328 results were not sensitive to the impact of potential outliers, nor were they sensitive to biased samples of
329 fish ages 1 and 2. In both cases, excluding these records changed estimates of K and L_∞ by less than half
330 a percentage point compared with their original values (Supplementary Table A1).

331 **4. Discussion**

332 Growth parameterization for the western stock of Atlantic bluefin tuna was substantially improved
333 by (1) adopting ageing protocols and data filtering criteria that reduced bias in both length increment
334 data and otolith-based ageing, (2) a large and more representative sample of age estimates than existed
335 historically, and (3) application of the AMSFc maximum likelihood approach, which allowed robust
336 weighting of tagging and otolith data (i.e., the results were not sensitive the relative weights placed on
337 the tagging and otolith likelihoods) in their combined use in parameterization of growth models.
338 Further, applying the more general Schnute model fitting approach allowed us to identify past process
339 error associated with adopting the traditional von Bertalanffy model. Because the observation and
340 process errors identified in our study are general to other migratory stocks, we suggest the complement
341 of approaches taken here for the western stock of ABT may serve to improve growth parameterization
342 across a range of exploited species.

343 Our new assessment of the ICCAT tag recapture data set and improvements to the growth curve
344 indicate that western ABT attain lower mean asymptotic sizes than previously thought. The Richards
345 parameterization of the Schnute model led to a better fit to the data. The shape parameter allowed it
346 more flexibility in fitting to the older ages, resulting in a lower estimate of L_∞ (271.0 cm FL) compared
347 to the von Bertalanffy parameterization (318.9 cm FL). This new estimate of the average size of fish in
348 the oldest age group appears to be in agreement with the range of maximum sizes reported in the
349 literature. In a recent meta-analysis of historical size data, Cort et al. (2013) uncovered a collection of
350 maximum sizes recorded during recreational fisheries competitions that took place between 1870 and
351 1979, and found record sizes of landed fish ranging from 210 to 320 cm FL (mean=269cm FL; where
352 the 320cm measurement was estimated from weight). Cort et al. (2013) also showed that records of fish
353 with lengths greater than 330cm FL in the ICCAT tagging database did not agree with the accepted
354 length-weight relationship, and were most likely the result of estimation errors or data misrecordings.
355 Looking exclusively at measured lengths, the 20 largest fish present in the database ranged from 246 to
356 295cm FL. According to the Richards model fit, an estimated variability in size-at-age of 21 cm near the
357 maximum age means we should expect 95% of old fish to reach sizes between 229 and 313 cm FL. This
358 result appears to be a more reasonable finding than that suggested by the von Bertalanffy fit which
359 implies that the oldest fish commonly reach maximum sizes between 261 and 377 cm FL.

360 Because otolith samples used in our analysis were largely obtained during fishery dependent
361 surveys, they are expected to reflect the selectivity of the fishery from which they were obtained
362 (Kolody et al. 2016; Schueller et al. 2014). Some of this sampling bias may have been lessened by large
363 sample size, particularly in comparison to Restrepo et al. (2010). Still, there was a noticeable lack of
364 very young fish in the otolith data (Fig. 1) that was likely due, in part, to the presence of a minimum
365 weight regulation of 30kg (~115cm FL) in the commercial fishery (in place since 1991) and, in part, to
366 difficulties associated with sampling the recreational fishery. Similarly, the positive trend in the
367 residuals of fish aged 1-3 apparent in both model fits (Fig. 2) could be a reflection of regulations placed
368 on the recreational fishery, which prohibits landing fish <27" curved fork length (~70cm FL). It is also

369 likely to be a reflection of seasonal growth. All samples for fish ages 1-3 were obtained in the summer
370 months (July-October for ages 1 and 2, and May-October for age 3) compared with other ages where,
371 depending on the age, 1-50% of samples were obtained during the winter months (Supplementary Fig.
372 A2). Faster growth in the summer has been recorded in the closely related species of southern bluefin
373 tuna (Eveson et al., 2004) for which seasonality in growth has been modeled, and is thus likely to occur
374 in ABT as well. Since seasonal changes in growth are most prominent in younger ages when fish
375 undergo rapid growth, it is likely that the positive trend in residuals is linked to the clustering of samples
376 age 1 and 2 around months of fastest growth.

377 Growth parameter estimates play a central role in the stock assessment of western Atlantic bluefin
378 tuna. They are needed to convert historical catch-at-size data into catch-at-age data, using cohort slicing,
379 and to estimate weight at age (ICCAT, 2014). Moreover, estimates of variability in size-at-age could be
380 used to improve the cohort slicing procedure by adjusting the length bounds used to assign ages to
381 individual fish. Preliminary analyses comparing cohort slicing results using growth parameters from the
382 two different models showed that the use of the Richards growth parameter estimates resulted in higher
383 contributions of very young and very old fish in the catch-at-age estimates compared with estimates
384 obtained using von Bertalanffy growth parameters. The extent to which this will have an impact on the
385 evaluation of the stock status is of prime interest and will need to be investigated. Growth parameter
386 estimates are also used to calculate spawning potential ratio and biological reference points.

387 Though a recent study by Siskey et al. (2016) suggests western ABT may have experienced subtle
388 differences in growth rates during the past four decades, it was unclear how much of the observed
389 changes might be due to fisheries selection or differences in sample coverage between decades (i.e., the
390 relative number of small vs. large fish in the sample). Further investigation into that issue is warranted
391 as using time-varying growth curves may help decrease uncertainty in the catch-at-age estimates used in
392 the assessment, particularly with retrospective approaches such as catch-at-age-analysis. However, until
393 balanced samples for each time period become available (perhaps through data mining of length
394 frequency data), it is best to continue the use a single growth curve in the stock assessment of western
395 ABT that is representative of the time period covered by the assessment as a whole.

396 Finally, there have been discussions in ICCAT about possibly moving towards a length-based
397 integrated assessment (ICCAT, 2014). If and when that happens, having good estimates of the average
398 length of the oldest age-class in the model (L_2) and variability in size at age will become crucial since
399 these parameters can play an important role in determining management outcomes (Aires-da-Silva et al.,
400 2015; Zhu et al. 2016). The observed differences in mean asymptotic length estimates are also likely to
401 affect assessment results. Having reliable estimates of L_∞ is particularly important for determining stock
402 productivity and associated reference points used for management advice (Aires-da-Silva et al., 2015;
403 Aires-da-Silva and Maunder, 2011) so further investigation should be carried out to determine the
404 importance of such a change.

405 **Acknowledgments**

406 We would like to thank Chris Francis and Mark Maunder for their help with coding in ADMB-RE,
407 and Alain Fonteneau for helpful suggestions on an earlier draft. A special thanks goes out to all the
408 fishermen who, through their cooperation, made this analysis possible. We would also like to thank the
409 Large Pelagics Research Center for their help acquiring samples in 2011. Financial support was
410 provided by the NOAA National Marine Fisheries Service Bluefin Tuna Research Program as well as a
411 NMFS/Sea Grant Fellowship in Population and Ecosystem Dynamics to LEA. This research was carried
412 out (in part) under the auspices of the Cooperative Institute for Marine and Atmospheric Studies, a
413 cooperative institute of the University of Miami, and the National Oceanic and Atmospheric

414 Administration (cooperative agreement NA17RJ1226). This paper is Contribution No. XXXX of the
415 Virginia Institute of Marine Science, College of William & Mary.

416

417 Appendix A. Supplementary data

418 Supplementary data associated with this article can be found, in the online version, at

419

420

421

422 References

423

424 Ailloud, L.E., Lauretta, M.V., Hoenig, J.M., Walter, J.F., Fonteneau, A., 2014. Growth of Atlantic
425 bluefin tuna determined from the ICCAT tagging database: A reconsideration of methods. Collect.
426 Vol. Sci. Pap. ICCAT 70, 380-393.

427 Aires-da-Silva, A.M., Maunder, M.N., Schaefer, K.M., Fuller, D.W., 2015. Improved growth estimates
428 from integrated analysis of direct aging and tag–recapture data: an illustration with bigeye tuna
429 (*Thunnus obesus*) of the eastern Pacific Ocean with implications for management. Fish. Res. 163,
430 119-126.

431 Aires-da-Silva, A.M., Maunder, M.N., 2011. Status of bigeye tuna in the Eastern Pacific Ocean in 2009
432 and outlook for the future. Inter-American Tropical Tuna Commission Stock Assessment Report 11,
433 17-156.

434 Block, B.A., Teo, S.L., Walli, A., Boustany, A., Stokesbury, M.J., Farwell, C.J., Weng, K.C., Dewar, H.,
435 Williams, T.D., 2005. Electronic tagging and population structure of Atlantic bluefin
436 tuna. Nature 434, 1121-1127.

437 Block, B.A., Dewar, H., Blackwell, S.B., Williams, T.D., Prince, E.D., Farwell, C.J., Boustany, A., Teo,
438 S.L., Seitz, A., Walli, A., Fudge, D., 2001. Migratory movements, depth preferences, and thermal
439 biology of Atlantic bluefin tuna. Science 293, 1310-1314.

440 Boustany, A.M., Reeb, C.A., Block, B.A., 2008. Mitochondrial DNA and electronic tracking reveal
441 population structure of Atlantic bluefin tuna (*Thunnus thynnus*). Mar. Biol. 156, 13-24.

442 Busawon, D.S., Rodriguez-Marin, E., Luque, P.L., Allman, R., Gahagan, B., Golet, W., Koob, E.,
443 Siskey, M.R., Sobrón, M.R., Quelle, P., Neilson, J., Secor, D.H., 2015. Evaluation of an Atlantic
444 Bluefin Tuna Otolith Reference Collection. Collect. Vol. Sci. Pap. ICCAT 71, 960-982.

445 Carlsson, J., McDowell, J.R., Carlsson, J.E., Graves, J.E., 2007. Genetic identity of YOY bluefin tuna
446 from the eastern and western Atlantic spawning areas. J. Hered. 98, 23-28.

447 Collette, B.B., Nauen, C.E., 1983. FAO Species Catalogue. Vol. 2. Scombrids of the world. An
448 annotated and illustrated catalogue of tunas, mackerels, bonitos and related species known to date.
449 Rome: FAO. FAO Fish. Syn. 125, 137 p.

450 Cort, J.L., Deguara, S., Galaz, T., Mèlich, B., Artetxe, I., Arregi, I., Neilson, J., Andrushchenko, I.,
451 Hanke, A., Neves dos Santos, M., Estruch, V., 2013. Determination of L max for Atlantic Bluefin
452 Tuna, *Thunnus thynnus* (L.), from meta-analysis of published and available biometric data. Rev.
453 Fish. Sci. 21, 181-212.

454 Eveson, J.P., Laslett, G.M., Polacheck, T., 2004. An integrated model for growth incorporating tag
455 recapture, length frequency, and direct aging data. Can. J. Fish. Aquat. Sci. 61, 292-306.

456 Fabens, A.J., 1965. Properties and fitting of the von Bertalanffy growth curve. Growth 29, 265-289.

457 Francis, R.C., Aires-da-Silva, A.M., Maunder, M.N., Schaefer, K.M., Fuller, D.W., 2016. Estimating
458 fish growth for stock assessments using both age–length and tagging-increment data. Fish. Res. 180,
459 113-118.

460 Francis, R.I.C.C., 1988. Are growth parameters estimated from tagging and age-length data
461 comparable? Can. J. Fish. Aquat. Sci. 45, 936-942.

462 Fournier, D.A., Skaug, H.J., Ancheta, J., Ianelli, J., Magnusson, A., Maunder, M.N., Nielsen, A., Sibert,
463 J., 2012. AD Model Builder: using automatic differentiation for statistical inference of highly
464 parameterized complex nonlinear models. Optim. Method. Softw. 27, 233-249.

465 ICCAT, 2014. Report of the 2014 ICCAT Atlantic bluefin tuna stock assessment session. Collect. Vol.
466 Sci. Pap. ICCAT 71, 692-945.

467 Kolody, D.S., Eveson, J.P., Hillary, R.M., 2016. Modelling growth in tuna RFMO stock assessments:
468 Current approaches and challenges. *Fish. Res.* 180, 177-193.

469 Laslett, G.M., Eveson, J.P., Polacheck, T., 2002. A flexible maximum likelihood approach for fitting
470 growth curves to tag recapture data. *Can. J. Fish. Aquat. Sci.* 59, 976-986.

471 Maunder, M.N. and Punt, A.E., 2013. A review of integrated analysis in fisheries stock
472 assessment. *Fish. Res.* 142, 61-74.

473 Neilson, J.D., Campana, S.E., 2008. A validated description of age and growth of western Atlantic
474 bluefin tuna (*Thunnus thynnus*). *Can. J. Fish. Aquat. Sci.* 65, 1523-1527.

475 Palmer, M.J., Phillips, B.F., Smith, G.T., 1991. Application of nonlinear models with random
476 coefficients to growth data. *Biometrics* 47, 623-635.

477 Restrepo, V.R., Diaz, G.A., Walter, J.F., Neilson, J.D., Campana, S.E., Secor, D., Wingate, R.L., 2010.
478 Updated estimate of the growth curve of western Atlantic bluefin tuna. *Aquat. Living Resour.* 23,
479 335-342.

480 Richards, F.J., 1959. A flexible growth function for empirical use. *J. Exp. Bot.* 10, 290-301.

481 Richardson, D.E., Marancik, K.E., Guyon, J.R., Lutcavage, M.E., Galuardi, B., Lam, C.H., Walsh, H.J.,
482 Wildes, S., Yates, D.A., Hare, J.A., 2016. Discovery of a spawning ground reveals diverse migration
483 strategies in Atlantic bluefin tuna (*Thunnus thynnus*). *Proc. Natl. Acad. Sci. U.S.A.* 113, 3299-3304.

484 Riccioni, G., Landi, M., Ferrara, G., Milano, I., Cariani, A., Zane, L., Sella, M., Barbujani, G., Tinti, F.,
485 2010. Spatio-temporal population structuring and genetic diversity retention in depleted Atlantic
486 bluefin tuna of the Mediterranean Sea. *Proc. Natl. Acad. Sci. U.S.A.* 107, 2102-2107.

487 Rodriguez-Marin, E., Ortiz, M., de Urbina, J.M.O., Quelle, P., Walter, J., Abid, N., Addis, P., Alot, E.,
488 Andrushchenko, I., Deguara, S., Di Natale, A., 2015. Atlantic Bluefin Tuna (*Thunnus thynnus*)
489 *Biometrics and Condition*. *PloS one* 10, p.e0141478.

490 Schnute, J., 1981. A versatile growth model with statistically stable parameters. *Can. J. Fish. Aquat.*
491 *Sci.* 38, 1128-1140.

492 Schnute, J., Fournier, D., 1980. A new approach to length-frequency analysis: growth structure. *Can. J.*
493 *Fish. Aquat. Sci.* 37, 1337-1351.

494 Secor, D.H., Allman, R., Busawon, D., Gahagan, B., Golet, W., Koob, E., Luque, P.L., Siskey, M.,
495 2014a. Standardization of otolith-based ageing protocols for Atlantic bluefin tuna. *Collect. Vol. Sci.*
496 *Pap. ICCAT* 70, 357-363.

497 Secor, D.H., Busawon, D.S., Gahagan, B., Golet, W., Koob, E., Neilson, J.D., Siskey, M., 2014b.
498 Conversion factors for Atlantic bluefin tuna fork length from measures of snout length and otolith
499 mass. *Collect. Vol. Sci. Pap. ICCAT* 70, 364-367.

500 Secor, D.H., Wingate, R.L., Neilson, J.D., Rooker, J.R., Campana, S.E., 2009. Growth of Atlantic
501 bluefin tuna: direct age estimates. *Collect. Vol. Sci. Pap. ICCAT* 64, 405-416.

502 Secor, D.H., 2007. The year class phenomenon and the storage effect in marine fishes. *J. Sea Res.* 57,
503 91-103.

504 Schueller, A.M., Williams, E.H., Cheshire, R.T., 2014. A proposed, tested, and applied adjustment to
505 account for bias in growth parameter estimates due to selectivity. *Fish. Res.* 158, 26-39.

506 Sibert, J.R., Lutcavage, M.E., Nielsen, A., Brill, R.W., Wilson, S.G., 2006. Interannual variation in
507 large-scale movement of Atlantic bluefin tuna (*Thunnus thynnus*) determined from pop-up satellite
508 archival tags. *Can. J. Fish. Aquat. Sci.* 63, 2154-2166.

509 Siskey, M.R., Wilberg, M.J., Allman, R.J., Barnett, B.K., Secor, D.H., 2016. Forty years of fishing:
510 changes in age structure and stock mixing in northwestern Atlantic bluefin tuna (*Thunnus thynnus*)
511 associated with size-selective and long-term exploitation. *ICES J. Mar. Sci.* 73, 2518-2528.

- 512 Skaug, H., Fournier, D., 2015. Random Effects in AD Model Builder. ADMB-RE User Guide Version
513 11.4.1, Available from: <http://www.admb-project.org/documentation/manuals> (accessed 31.05.16).
- 514 Turner, S.C., Restrepo, V.R., 1994. A review of the growth rate of west Atlantic bluefin tuna, *Thunnus*
515 *thynnus*, estimated from marked and recaptured fish. Collect. Vol. Sci. Pap. ICCAT 42, 170-172.
- 516 Von Bertalanffy, L., 1938. A quantitative theory of organic growth (inquiries on growth laws. II). Hum.
517 Biol. 10, 181-213.
- 518 Wang, Y.G., Thomas, M.R., Somers, I.F., 1995. A maximum likelihood approach for estimating growth
519 from tag-recapture data. Can. J. Fish. Aquat. Sci. 52, 252-259.
- 520 Zhu, J., Maunder, M.N., Aires-da-Silva, A.M., Chen, Y., 2016. Estimation of growth within Stock
521 Synthesis models: Management implications when using length-composition data. Fish. Res. 180,
522 87-91.

523
524
525
526
527
528
529
530
531
532
533
534
535
536
537
538
539
540
541
542
543
544
545
546
547
548
549

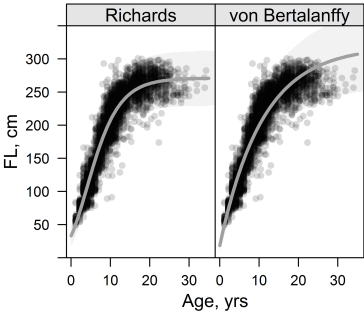
Figure 1. Otolith data plotted against the fitted Richards and von Bertalanffy curves (grey solid lines). In each panel, the shaded area represents the 2.5 and 97.5 percentiles of the distribution of the fitted length at age.

Figure 2. Scatterplot of otolith standardized residuals resulting from the Richards and von Bertalanffy model fits. A loess line (grey solid line) was fitted to the residuals in each panel to investigate trends. For reference, horizontal dotted lines are drawn at 0 and ± 2 standardized residuals.

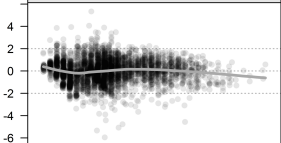
Figure 3. Tagging data plotted against the fitted Richards and von Bertalanffy curves (grey solid lines). Each vector represents the growth trajectory of a fish given its known length at release, length at recapture, time spent at liberty and estimated age at tagging (estimated using empirical Bayes methods). In each panel, the shaded area represents the 2.5 and 97.5 percentiles of the distribution of the fitted length at age.

Figure 4. Estimated frequency (histogram) and probability density function (grey solid line) of the lognormal distribution of the random effects for the Richards and the von Bertalanffy models.

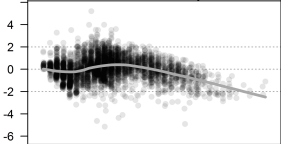
Figure 5. Quantiles in distribution of $(L_{rec}|L_{tag}, \Delta t)$ for the Richards and von Bertalanffy models. If the data were well fitted, the histogram of quantiles would follow an approximately uniform distribution and lie close to the horizontal dotted line.



Richards



von Bertalanffy



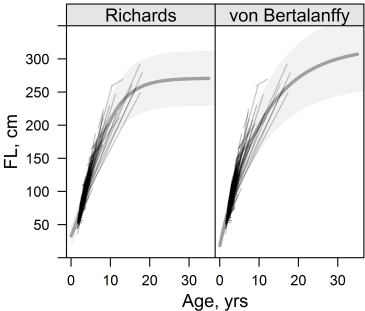
0

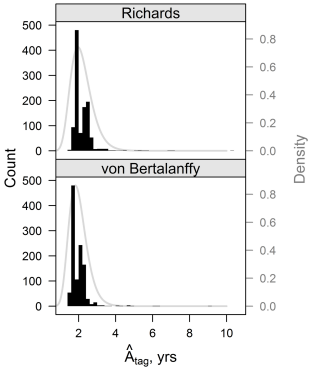
10

20

30

Age, yrs





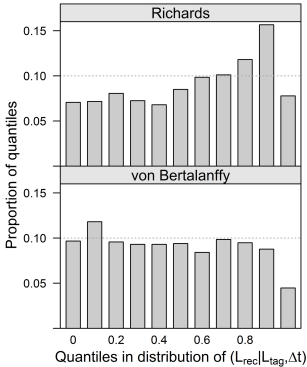


Table 1. Maximum likelihood estimates for the parameters of the Richards and von Bertalanffy growth models. Note: the K parameters of the Schnute parameterization of the Richards and von Bertalanffy models have different interpretations (see methods section 2.4).

	Richards (Schnute with $p < 1$)		Von Bertalanffy (Schnute with $p = 1$)	
	Value	S.E.	Value	S.E.
Fixed parameters				
A_1	0	-	0	-
A_2	34	-	34	-
p	-	-	1	-
Estimated parameters				
L_1	33.0	0.74	18.5	1.1
L_2	270.6	1.3	305.9	1.8
K	0.22	0.01	0.09	0.002
p	-0.12	0.05	-	-
k_ρ	1.5	0.18	0.97	0.15
ρ_0	0.97	0.01	0.94	0.01
σ_{obs}	3.6	0.46	2.8	0.44
σ_{L_1}	7.7	0.60	5.0	0.66
σ_{L_2}	21.0	0.69	29.1	0.91
$\mu_{logAtag}$	0.74	0.02	0.66	0.02
$\sigma_{logAtag}$	-1.3	0.04	-1.4	0.05
Derived parameters				
L_∞	271.0	1.39	318.9	2.56
t_0	0	-	-0.65	0.05
a^*	5.84	0.69	3.5	0.75
b	0.06	0.004	0.08	0.004
Negative log-likelihood	19597.1		19884.7	